FINITE ELEMENT COMPUTATIONS OF TIME RELAXATION ALGORITHM FOR FLOW ENSEMBLES

Monika Neda[1*], Jiajia Waters[2]

[1]Department of Mathematical Sciences, University of Nevada Las Vegas, Las Vegas, NV, 89154-4020, USA.
[2] Los Alamos National Laboratory, T-3 Solid Mechanics and Fluid Dynamics, Los Alamos, New Mexico, USA.

Abstract:
Numerical continuous finite element computations of a fluid flow modelling based on ensemble technique are presented herein. This ensemble algorithm is based on time relaxation. At each time step, it requires the storage of a single coefficient matrix with multiple right-hands sides which corresponds to each ensemble member. Finite element convergence results for the time relaxation ensemble algorithm are presented and tested in a numerical experiment. This numerical experiment supports the theoretical finite element results. The time relaxation efficiency was shown in the second cavity benchmark problem.

ARTICLE HISTORY
Received 17 may 2016
Accepted 15 June 2016
Available online 30 june 2016

KEYWORDS
fluid dynamics, partial differential equations, finite element, simulation

1. INTRODUCTION

Numerous fluid flow applications require efficient calculations of ensembles for incompressible flow, see [1-2]. The quantification of uncertainties in forcing terms, initial and boundary conditions, constitutive laws, geometry of the domain and model parameters, see [3-8], involves ensembles. In general, ensemble forecasting uses a sample of randomly generated initial conditions based on some observations available. This is applied in numerical weather prediction, see [9], and in sensitivity analysis of forecast fields to initial conditions, see [10].

We start by considering the *J* solutions of Navier-Stokes equations (NSE) described by the following. Given initial condition u_j^0, and body force f_j solve for velocity u_j, and pressure p_j, for $1 \le j \le J$ satisfying

$$\frac{\partial u_j}{\partial t} + u_j \cdot \nabla u_j - \nu \Delta u_j + \nabla p_j = f_j(x,t) \ \ in \ \Omega, \qquad (1.1)$$

$$\nabla \cdot u_j = 0 \ \ in \ \Omega, \qquad (1.2)$$

$$u_j = 0 \ \ on \ \ \partial\Omega, \qquad (1.3)$$

$$u_j(x,0) = u_j^0(x) \ \ in \ \ \Omega. \qquad (1.4)$$

where Ω represents the domain of the problem of interest and $\partial\Omega$ its boundary. When solving (1.1)-(1.4) by linearly implicit methods, the linear solve step is often the most computationally expensive step with respect to the needed memory and turnaround time. If a brute-force approach is used for (1.1)-(1.4) by running *J* simulations consecutively, it would increase the turnaround time by a factor of *J*. In [1], a method for computing the ensemble in one run was proposed for low *Re* number flows by Layton and Jiang. Motivated by that study, in [11] a study of an ensemble method for higher Re flows was presented. This method was obtained by adapting the time relaxation model of NSE to the ensemble calculation of (u_j, p_j)'s. Now we present the time relaxation model that was first introduced by Stolz, Adams and Kleiser [12-14]. Thereafter, it was extensively studied in [15-18]. This time relaxation model is obtained by adding a linear time regularization term, χu^* to NSE, yielding

$$\frac{\partial u}{\partial t} + u \cdot \nabla u - \nu \Delta u + \nabla p + \chi u^* = f(x,t) \ \ in \ \ \Omega, \qquad (1.5)$$

$$\nabla \cdot u = 0 \ \ in \ \ \Omega, \qquad (1.6)$$

$$u = 0 \ \ on \ \ \partial\Omega, \qquad (1.7)$$

$$u(x,0) = u^0(x) \ \ in \ \ \Omega, \qquad (1.8)$$

CONTACT: Monika Neda, monika.neda@unlv.edu.

where u is velocity, p is pressure, f is the body force, u^0 is the initial condition and u^* is a generalized fluctuation. Here, the units for $[\chi]=\frac{1}{time}$. Overall, one can apply any local spatial and time averages [19, 20] of the velocity field for $\bar{u}$. Within the theory of the ensemble algorithm u^* can be computed directly as

$$u_j^* = u_j - \bar{u},$$

where for $g_j, j=1...,J,$ we define the ensemble mean as

$$\bar{g} := \frac{1}{J}\sum_{j=0}^{j} g_j.$$

After suppressing the spatial discretization, the time relaxation ensemble calculation method is described as:

Algorithm 1.1. Find $\left(u_j^{n+1}, p_j^{n+1}\right)$, with J initial velocities u_j^0 and forcing terms f_j, and parameter $\chi = O\left(\frac{1}{\Delta t}\right) \geq 0$, satisfying

$$\frac{u_j^{n+1}-u_j^n}{\Delta t} + \overline{u^n}\cdot\nabla u_j^{n+1} + \left(u_j^n - \overline{u^n}\right)\cdot\nabla u_j^n + \nabla p_j^{n+1}$$

$$-v\Delta u_j^{n+1} + \chi\left(u_j^{n+1} - \overline{u^n}\right) = f_j\left(t^{n+1}\right), \qquad (1.9)$$

$$\nabla\cdot u_j^{n+1} = 0 \qquad (1.10)$$

The above Algorithm 1.1 can be rewritten in a more compact form as

$$\left(\frac{1}{\Delta t}+\chi\right)u_j^{n+1} + \overline{u^n}\cdot\nabla u_j^{n+1} + \nabla p_j^{n+1} - v\Delta u_j^{n+1} = RHS_j^{n+1},$$

$$\nabla\cdot u_j^{n+1} = 0,$$

In this form, it requires that only a single coefficient matrix is stored along with J right-hand sides. The natural choice of $\chi = O\left(\frac{1}{\Delta t}\right)$ for the Algorithm 1.1 is consistent with and supported by the stability result, see Lemma 3.1. The proposed time relaxation model is easily implementable in existing NSE codes. The proposed algorithm significantly reduces the required storage, especially for large number of ensembles J.

This paper is organized in few sections. Section 2 contains the preliminaries and the finite element discretization of the Algorithm 1.1. In sections 3, the finite element stability and the convergence of the method are stated. Next, Section 4 contains numerical experiments and a conclusion is given in the last section 5.

2. PRELIMINARIES

We denote by $\Omega \subset R^d$, $d = 2,3$ an open, simply connected domain with piecewise smooth boundary. Herein, we assume no-slip boundary conditions. The $L^2(\Omega)$ norm and inner product will be denoted by $\|\cdot\|$ and $(\cdot,\cdot)$, respectively. Then, the appropriate velocity and pressure spaces are defined as usual by

$X := \left(H_0^1(\Omega)\right)^d$, *and* $Q := L_0^2(\Omega)$, respectively.

The standard notation for the seminorm on $H^k(\Omega)$ is $|\cdot|_k$. The dual space $X^* = H^{-1}(\Omega)$ is equipped with the usual dual norm

$$\|f\|_{-1} = \sup_{v\in X}\frac{\langle f,\nabla v\rangle}{|v|_1},$$

The space of divergence free functions is given by

$$V := \left\{v \in X : (\nabla\cdot v,\ q) = 0,\ \forall q \in Q\right\}.$$

We assume that conforming finite element spaces $X_h \subset X$, $Q_h \subset Q$ satisfy the usual inf-sup stability condition [7]. The space of weakly divergence free functions is denoted by

$$V_h := \left\{v_h \in X_h : (\nabla\cdot v_h,\ q_h) = 0,\ \forall_{qh} \in Q_h\right\}.$$

The skew-symmetrized trilinear form is defined in the usual way

$$b^*(u,v,w) = \frac{1}{2}(u\cdot\nabla v, w) - \frac{1}{2}(u\cdot\nabla w, v). \qquad (2.1)$$

Definition 2.1. For any norm space Y, the fluctuation in j-th ensemble member g_j, and the norm $\|g\|_Y$ are defined as $g_j' := g_j - \bar{g}$ and $\|g\|_Y^2 := \frac{1}{J}\sum_{j=1}^{J}\|g_j\|_Y^2$, respectively. Further, we set $\|g\|_{m,k} := \max_{1\leq j\leq J}\|g_j\|_{L^m(0,T;H^k(\Omega))}$. With this notation $\|\bar{g}\|_Y \leq \|g\|_Y$ and $\|g'\|_Y = \sqrt{\sum_{j=1}^{J}\|g_j'\|_Y^2} \leq 2\|g\|_Y$.

We next introduce the weak finite element formulation of our model based on continuous finite element methodology and notation introduced above.

Algorithm 2.2. Find $\left(u_{j,h}^{n+1}, p_{j,h}^{n+1}\right) \in (X_h, Q_h)$, $n = 0,1...,N-1$ with J initial velocities u_j^0 and forcing terms $f_j \in H^{-1}(\Omega)$, a time step $\Delta t_{n+1} > 0$, and

parameter $\chi_{n+1}=\frac{c_\chi}{\Delta t_{n+1}}$ for some $C_\chi=O(1)\geq 0$, satisfying

$$\frac{1}{\Delta t_{n+1}}\left(u_{j,h}^{n+1}-u_{j,h}^{n},v_h\right)+b^*\left(\overline{u_h^n},u_{j,h}^{n+1},v_h\right)+$$
$$b^*\left(u_{j,h}^{n}-\overline{u_h^n},u_{j,h}^{n},v_h\right)-\left(p_{j,h}^{n+1},\nabla\cdot v_h\right)+\nu\left(\nabla u_{j,h}^{n+1},\nabla v_h\right)+ \quad (2.2)$$
$$\chi_{n+1}\left(u_{j,h}^{n+1}-\overline{u_h^n},v_h\right)=\left\langle f_j\left(t^{n+1}\right),v_h\right\rangle,\forall v_h\in X_h,$$
$$\left(\nabla\cdot u_{j,h}^{n+1},q_h\right)=0,\ \forall q_h\in Q_h. \quad (2.3)$$

3. FINITE ELEMENT STUDY

In this section, we present the stability and convergence results. They are obtained under a time step condition defined below

$$\frac{4\Delta t_{n+1}}{\nu}\left(\left\|u_{j,h}^{n'}\right\|_\infty^2+\left\|\nabla\cdot u_{j,h}^{n'}\right\|_\infty^2\frac{diam(\Omega)^2}{d^2}\right)\leq 1,\forall_j=1,...,J, \quad (3.1)$$

where $d=2,3$ is the space dimension. This time step condition is satisfied provided the fluctuations are small enough at each time step. Moreover, if the space of weakly divergence free functions is conforming, i.e., $V_h\in V$, then (3.1) reduces to a weaker condition

$$\frac{4\Delta t_{n+1}}{\nu}\left\|u_{j,h}^{n'}\right\|_\infty^2\leq 1,\forall_j=1,...,J. \quad (3.2)$$

since $\left\|\nabla\cdot u_{j,h}^{n'}\right\|_\infty^2=0$

Proposition 3.1. If for each time step $n\geq 1$, the condition (3.1) holds and $\chi_{n+1}=\frac{C_x}{\Delta t_{n+1}}$, then the numerical solutions to Algorithm 2.2 satisfy

$$\left\|u_h^N\right\|^2+C_x\left\|\overline{u_h^N}\right\|^2+\frac{\nu}{2}\sum_{n=0}^{N-1}\Delta t_{n+1}\left|u_h^{n+1}\right|_1^2+C_x\sum_{n=0}^{N-1}\left(2\left\|u_h^{n+1'}\right\|^2+\left\|\overline{u_h^{n+1}}-\overline{u_h^n}\right\|^2\right)$$
$$\leq\frac{1}{\nu}\sum_{n=0}^{N-1}\Delta t_{n+1}\left\|f\left(t^{n+1}\right)\right\|_{-1}^2+\left\|u_h^0\right\|^2+C_x\left\|\overline{u_h^0}\right\|^2. \quad (3.3)$$

Remark 3.2. This bound shows that the norm of the numerical finite element velocity solution will not change much under the change in data, i.e. body force, initial conditions and model parameters.

Proof. The proof is derived with all details in [11].

Next, we present the convergence results. Let $\left(X_h,Q_h\right)=\left(P_{k+1},P_k\right),k\geq 1$, be the Taylor-Hood finite element pair.

Theorem 3.3. Letting $e_j^n:=u_j^n-u_{j,h}^n$, the solutions of the discrete Algorithm 2.2 satisfy the following error estimate under some regularity assumptions

$$\left\|e^N\right\|^2+\nu\sum_{n=0}^{N-1}\Delta t_{n+1}\left|e^{n+1}\right|_1^2+C_x\sum_{n=0}^{N-1}\left\|e^{n+1'}\right\|^2+C_x\left\|\overline{e^N}\right\|^2$$
$$\leq C(\nu,T)\left(h^{2k}+\Delta t_{max}^2+C_x\sum_{n=0}^{N-1}\left\|u^{n+1'}\right\|^2\right) \quad (3.4)$$

Proof. The proof is derived with all details in [11].

Remark 3.4. The error estimate yields usual exponential dependence on the final time *T*, which arises from the application of Gronwall's inequality. This bound shows that the numerical finite element velocity solution will converge to the true Navier-Stokes velocity solution as we refine the mesh, i.e. as we let $h\to 0$. If *k* = 1, i.e. we are using P_2,P_1 finite element spaces, and $C_x=0$ we obtain second order of convergence in space and time. This is tested in the numerical experiment section.

4. NUMERICAL COMPUTATIONS

We test our numerical algorithm for convergence first using the Green-Taylor problem and then we applied it for the benchmark cavity problem.

4.1. Green-Taylor vortex solutions

Herein, we confirm the predicted convergence rates for generalized Green-Taylor vortex solutions, see [22]. The true solution of this problem is given by

$$u=\begin{pmatrix}\left(sin(5y)+cos(3x)cos(4y)\right)sin(-25\nu t)\\ \left(3/4\,sin(3x)sin(4y)+cos(5x)\right)sin(-25\nu t)\end{pmatrix},$$

$\nabla p=-u\cdot\nabla u$, and

$$f=\begin{pmatrix}-25\nu\left(sin(5y)+cos(3x)cos(4y)\right)\left(cos(-25\nu t)-\right.\\ -25\nu\left(3/4\,sin(3x)sin(4y)+cos(5x)sin\right)\left(cos(-25\nu t)-\right.\\ \left.-sin(-25\nu t)\right)\\ \left.-sin(-25\nu t)\right)\end{pmatrix}.$$

The square shaped domain $\Omega=(0,5)^2$ We also have the following parameters: viscosity $\nu=0.01$, final time $T=1$ and $C_x=0$ The numerical solutions were computed with $\left(P_2,P_1\right)$ Taylor-Hood finite element pair (i.e. second order polynomial approximations for velocity and first order polynomial approximations for pressure) on

successively refined meshes with corresponding values of time step Δt. The exact velocity solution of this numerical experiment is presented in Figure 4.1 at time $T=1$.

Initial conditions and the body forces for the ensemble members. For simplicity we take the number of ensemble members $J=2$. We generate initial conditions and source terms for the ensemble members as follows. Let $\varepsilon = 1e-5$, $\phi_1 = sin(200x)$, and $\phi_2 = cos(300y)$. Set

$$u_1^0 = u(x,0) + \varepsilon(\phi_1,\phi_2)^T, u_2^0 = u(x,0) - \varepsilon(\phi_1,\phi_2)^T,$$

$$f_1 = f - \varepsilon\nu\begin{pmatrix}\Delta\phi_1\\ \Delta\phi_2\end{pmatrix} + \varepsilon\begin{pmatrix}\phi_1\\ \phi_2\end{pmatrix}\cdot\nabla u + \varepsilon u\cdot\nabla\begin{pmatrix}\phi_1\\ \phi_2\end{pmatrix} + \varepsilon^2\begin{pmatrix}\phi_1\\ \phi_2\end{pmatrix}\cdot\nabla\begin{pmatrix}\phi_1\\ \phi_2\end{pmatrix}$$

$$f_2 = f + \varepsilon\nu\begin{pmatrix}\Delta\phi_1\\ \Delta\phi_2\end{pmatrix} - \varepsilon\begin{pmatrix}\phi_1\\ \phi_2\end{pmatrix}\cdot\nabla u - \varepsilon u\cdot\nabla\begin{pmatrix}\phi_1\\ \phi_2\end{pmatrix} + \varepsilon^2\begin{pmatrix}\phi_1\\ \phi_2\end{pmatrix}\cdot\nabla\begin{pmatrix}\phi_1\\ \phi_2\end{pmatrix}$$

It can be verified that $u_j = u \pm \varepsilon\begin{pmatrix}\phi_1\\ \phi_2\end{pmatrix}$, $p_j = -u\cdot\nabla u$, and the mean ensemble velocity $\bar{u}$ equals $u = \frac{u_1+u_2}{2}$.

When $C_x = 0$ and $\Delta t_n = \Delta t, \forall n$, error estimate (3.4) predicts second order convergence of the velocities. In all the runs performed, we start with $\Delta t_n = \frac{1}{h}$ and half the time step if the stability condition failed. Only when $h = 0.44$, the time step had to be refined 3 times.

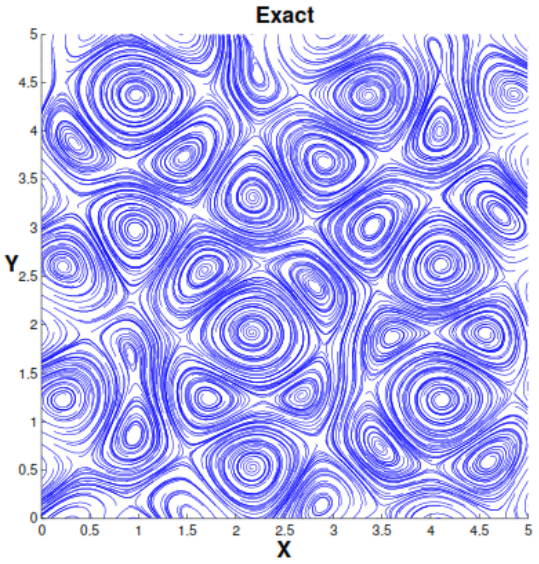

Fig. 4.1. Exact velocity solution at T = 1

Table 4.1. Error table for generalized Green-Taylor problem

h	$\|\|u_1 - u_{1,h}\|\|$	rate	$\|\|u_2 - u_{2,h}\|\|$	rate	$\|\|\bar{u} - \bar{u_h}\|\|$	rate
0.44	1.27913e-1	3.37	1.27837e-1	3.36	1.27836e-1	3.29
0.22	1.23822e-2	2.41	1.24348e-2	2.41	1.21608e-2	2.38
0.11	2.33631e-3	2.11	2.33686e-3	2.11	2.33205e-3	2.11
0.06	5.4255e-4	1.93	5.42808e-4	1.92	5.38684e-4	2.01
0.03	1.42443e-4	-	1.43048e-4	-	1.34003e-4	-

The results of the errors with the corresponding rate for the velocity are presented in Table 4.1.

The simulated velocity solution of this numerical experiment with $h = 0.88$ and $h = 0.44$ (from left to right) and the number of ensemble members $J = 2$ is presented in Figure 4.2 at time $T = 1$.

4.2. Lid driven cavity

The second problem we tested our algorithm with is lid driven cavity problem with viscosity $\nu = 1/1000$ on a square $[1.0,1.0]$ domain. The simulation is done on two different mesh sizes, $h = 1/10$ and $h = 1/20$, with $\chi = 1/\Delta t_n$ and $\chi = 0$. Time step Δt started with 0.01 and stability was not violated. Simulations are shown in Figures 4.3 and 4.4 at time $T = 5$, where we can see that for $h = 1/20$ and $\chi = 1/\Delta t_n$ the second recirculation is captured on the left corner while with $\chi = 0$ simulation has only one circulation on the right corner. See [24] for more comparison for lid driven cavity problem where a DNS method is implemented with $h = 1/31$ in order to capture both recirculation. When $h = 1/10$ the results are better with $\chi = 1/\Delta t_n$ than without χ.

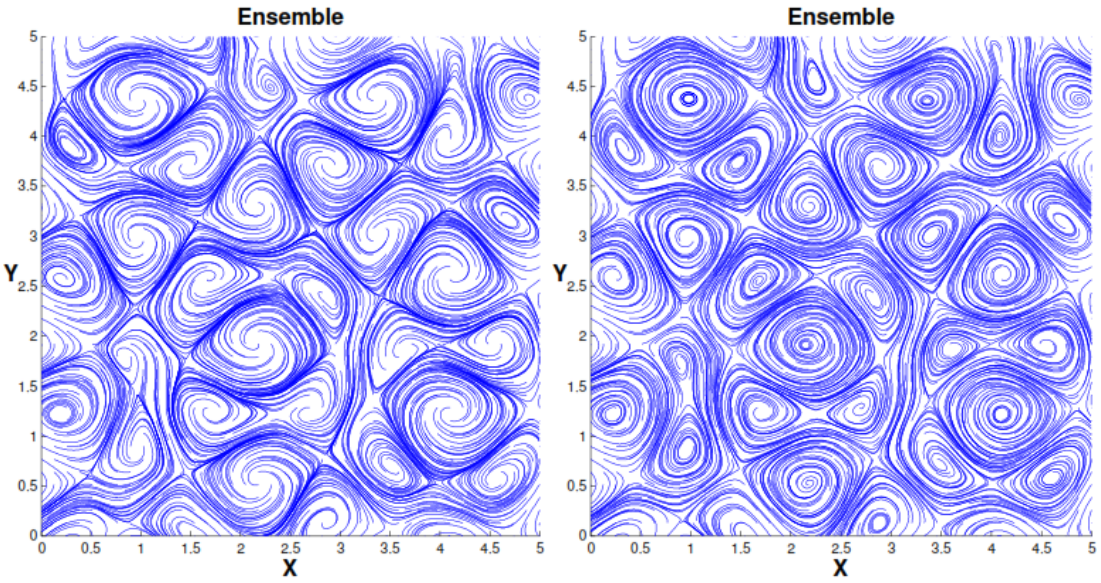

Fig. 4.2. Ensembled velocity solution at $T=1$ for $h=0.88$ and $h=0.44$ from left to right.

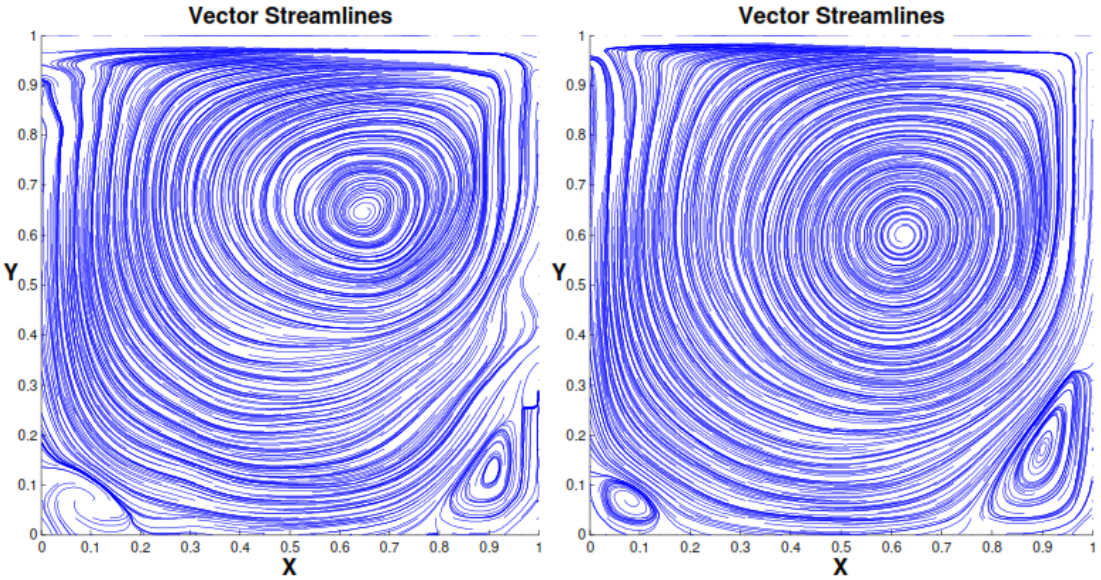

Fig. 4.3. Ensembled velocity solution with $\chi=1/\Delta t_n$ at $T=5$ (h = 1/10 and h = 1/20 from left to right, respectively).

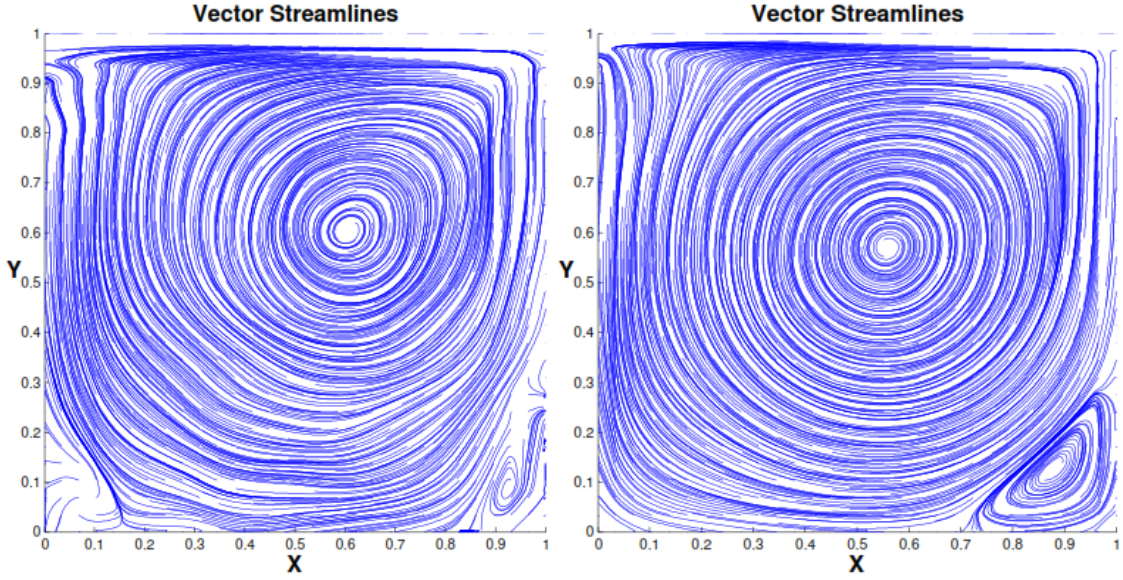

Fig. 4.4. Ensembled velocity solution with $\chi=0$ at $T=5$, ($h=1/10$ and $h=1/20$ from left to right, respectively).

5. CONCLUSIONS

Herein we presented a fluid model based on ensemble technique applied for the time relaxation regularization of NSE. This regularization acts to suppress the velocity fluctuations in a fluid flow by the means of ensemble methodology. Herein, we confirmed the theoretical rates of convergence of the true velocity solution towards the numerical finite element solution in the Green-Taylor numerical problem. In the second experiment, we showed the efficiency of the ensemble method and time relaxation on the cavity benchmark experiment.

REFERENCES

[1] N. Jiang, W. Layton, An algorithm for fast calculation of flow ensembles, International Journal for Uncertainty Quantification, 4 (2014), 273-301.

[2] M. Leutbecher, T. N. Palmer, Ensemble forecasting, J. Comp. Phys. 227 (2008), 3515-3539.

[3] C. Webster, G. Zhang, M. Gunzburger, An adaptive wavelet stochastic collocation method for irregular solutions of Stochastic Partial Diferential Equations, ORNL Tech. Rep., ORNL/TM- 2012/186, 2012.

[4] O. Le Matre, O. Knio, H. Najm, R. Ghanem, A stochastic projection method for fluid flow I. Basic formulation, J. Comput. Phys. 173 (2001), 481-511.

[5] P. Harasim, On the worst scenario method: Application to a quasilinear elliptic 2D-problem with uncertain coeficients, Appl. Math., 56(5) (2011), 459-480.

[6] L. G. Stanley, D. L. Stewart, Design Sensitivity Analysis: Computational Issues of Sensitivity Equation Methods, SIAM, Philadelphia, 2002.

[7] A. Saltelli, K. Chan, E. Scott eds., Sensitivity Analysis, Chichester, NY, Wiley, 2000.

[8] W. Oberkampf, J. Helton, Evidence theory for engineering applications, In Engineering Design Reliability Handook, ed. E Nikolaidis, D Ghiocel, S Singhal, pp. 130. Boca Raton, FL, CRC, 2005.

[9] Z. Toth, E. Kalnay, Ensemble Forecasting at NMC: The Generation of Perturbations, Bull. Amer. Meteor. Soc., 74(12), 1993, 2317-2330.

[10] W. J. Martin, M. Xue, Initial condition sensitivity analysis of mesoscale forecast using very-large ensembles, Mon. Wea. Rev., 134 (2006), 192-207.

[11] A. Takhirov, M. Neda, J. Waters, Time relaxation algorithm for ow ensembles, Numerical Methods for Partial Diffierential Equations, 32 (2016), 757-777.

[12] N.A. Adams, S. Stolz, An approximate deconvolution procedure for large eddy simulation, Phys. Fluids, 2 (1999), 1699-1701.

[13] N.A. Adams, S. Stolz, Deconvolution methods for subgrid-scale approximation in large eddy simulation, in: R.T. Edwards (Ed.), Modern Simulation Strategies for Turbulent Flow, Edwards, Philadelphia, 2001, p.21.

[14] N.A. Adams, S. Stolz, L. Kleiser, Approximate deconvolution model for large eddy simulation with application to wall-bounded ows, Phys. Fluids, 13(4) (2001), 997-1015.

[15] W. Layton, M. Neda, Truncation of scales by time relaxation, J. Math. Anal. Appl., 325 (2007), 788-807.

[16] C. D. Pruett, T. B. Gatski, C. E. Grosch, and W. D. Thacker, The temporally filtered Navier-Stokes equations: Properties of the residual stress, Phys. Fluids, 15(8) (2003), 2127-2140.

[17] S. Dee, D. Hannach, M. Neda, E. Nikonova, Numerical Analysis and Computations of a High Accuracy Time Relaxation Fluid Flow Model, Int. J. Comp. Math., 89 (2012), 2353-2373.

[18] M. Neda, Discontinuous Time Relaxation Method for the Time Dependent Navier-Stokes Equations, Adv. Numer. Anal., (2010), Article ID 419021, doi:10.1155/2010/419021.

[19] L. Berselli, T. Iliescu, W. Layton, Mathematics of large eddy simulation of turbulent ows, Springer, 2006.

[20] W. Layton, L. Rebholz, Approximate Deconvolution Models of Turbulence, Springer, 2012.

[21] V. Girault, P. A. Raviart, Finite element methods for Navier-Stokes equations: theory and algorithms, Springer, 1986.

[22] O. Walsh, Eddy solutions of the Navier-Stokes equations, The Navier-Stokes Equations II Theory and Numerical Methods, 1530 (1992), 306-309.

[23] J. Waters, D. W. Pepper Global Versus Localized RBF Meshless Methods for Solving Incompressible Fluid Flow with Heat Transfer, Numerical Heat Transfer, Part B: Fundamentals, 68(3) (2015), 185-203.